AIMS Mathematics, 11(1): 1927–1953.
DOI: 10.3934/math.2026080
Received: 11 October 2025
Revised: 05 January 2026
Accepted: 12 January 2026
Published: 21 January 2026

https://www.aimspress.com/journal/Math

Research article

Multiple rumor source localization in signed social networks driven by data intelligence

Ying Guo[1] and Yong-nan Li[1,2,*]

[1] School of National Security, People's Public Security University of China, Beijing 100038, China
[2] Intelligent Policing and National Security Risk Management Laboratory, Luzhou 646000, China

* **Correspondence:** Email: liyongnan@ppsuc.edu.cn.

Abstract: With the help of deepfake algorithms and social bots, the problems of consciousness penetration and cognitive manipulation caused by the outbreak of internet rumors have become prominent. Accurately locating the rumor sources and quickly cutting off the critical paths of rumor propagation will become an effective ways to curb the explosive spread of rumors and the sudden accumulation of negative emotions. In this paper, we combine the complementary advantages of signed graph convolutional networks in spatial and spectral domains, propose an improved multirumor source localization framework for signed social networks, and extend the rumor centrality principle and source prominence theory to the scope of signed networks. First, structural balance theory is used to accurately model positive and negative social relations. Second, a signed graph convolutional network based on signed attention mechanism is proposed to extract the rumor centrality feature from the infection subgraph. Then, a two-stream graph convolutional network based on a label propagation mechanism is proposed to extract the source prominence feature from the subgraph containing only positive edges and the subgraph containing only negative edges, respectively. Finally, the center feature of the infected structure and the position distribution feature of infected and uninfected nodes are integrated in a unified framework for multirumor source localization. Extensive experimental results on four real-world social network datasets show that compared with state-of-the-art algorithms, our proposed algorithm further improves the accuracy and robustness in the task of multiple rumor source localization.

Keywords: rumor source localization; signed graph convolutional network; signed attention mechanism; label propagation; two-stream network

Mathematics Subject Classification: 68T20, 68T37, 91D30, 91E10

1. Introduction

The problem of source node localization is to infer the initial infection sources in the network according to one snapshot of the infection state of all nodes at a certain time [1]. Because there may be one or more infection sources, the source localization problem is further divided into single-source localization and multisource localization. Most of the current research ideas are to combine node infection status and network topology for source localization. Multiple rumor source localization (MRSL) determines the location of multiple rumor sources in the context of online social networks. Internet rumors spread rapidly, often with emotional polarity, and even containing ideological views which may erode mainstream values, lead to social trust crisis, and threaten national political security. Therefore, rumor source localization has increasingly become a hotbed for research activity [2].

There are several possible solutions to the problem of MRSL. The first approach is from the perspective of complex networks: the source centrality index is proposed, and the center of the infection subgraph is defined as the source node. Common methods include rumor centrality [3], a combination of eccentricity and closeness centrality [4], and so on. However, these methods are unable to dynamically model the propagation process. The second approach is from the perspective of diffusion models, proposing models suitable for online social networks. Existing diffusion models are usually divided into two categories: influence models and infection models [5]. Common influence models include the independent cascade (IC) model and the linear threshold (LT) model, while common infection models include the susceptible–infected (SI) model and the susceptible–infected–recovered (SIR) model. Due to the prevalence of emotional polarity in social networks, Zhang et al. [6] proposed an asymmetric flip cascade (MFC) model based on signed social networks, considering the asymmetry of the influence of positive and negative edges on information dissemination. They increased the activation probability of positive edges through the asymmetric boosting coefficient and then extracted a set of the roots of infection cascade trees as the rumor source set. Li et al. [7] incorporated the theory of social psychology to calculate the infection probability of positive and negative edges, respectively, and constructed the signed-SI (S-SI) model for epidemic spreading dynamics on signed social networks. Jiang et al. [1] proposed a signed-SIR (S-SIR) model to adapt to signed networks and used an improved message passing algorithm for source identification. However, these methods require the diffusion model as prior knowledge.

A third approach, from the perspective of label propagation, multisource rumor localization is conducted by using the source prominence theory without knowing the underlying diffusion model. Wang et al. [8] were the first to propose label propagation-based source identification (LPSI). At first, each node is assigned an initial label value. After that, their label values are propagated and updated iteratively. Finally, the convergence result is obtained, where the local maximum points are identified as the source nodes. Subsequently, many variants of the LPSI algorithm emerged. Ma et al. [9] combined the direction-induced search (DIS) and LPSI algorithms and proposed the DISLPSI framework, which adaptively selects observer nodes by the adaptive observation node selection (AONS) algorithm. First, observer nodes are dynamically selected to record the propagation direction. Then, the source nodes are traced back through iterative search. However, observer-based source localization methods not only have performance directly related to the selection of observer nodes but also require additional information beyond network snapshots such as the infection paths (i.e., the neighbors that sent the information) and infection times (i.e., the times when the information was

received) recorded by the observer nodes. Such information is often difficult to obtain in real-world social networks, however.

A fourth approach, from the perspective of backpropagation, source localization is regarded as the inverse of information dissemination, and the backpropagation algorithm is utilized to detect the source node. Qiu et al. [10] proposed a single-source localization method (BPSL) applicable to general networks which takes into account both infection structure and time delay. First, they put forward an observer selection strategy based on maximizing influence to minimize the number of observers. Second, they proposed a source localization method using the reverse propagation of timestamps. However, this algorithm assumes that the transmission probabilities of all edges are the same. Ma et al. [11] first proposed a single-source localization method for signed networks, taking into account both the propagation structure and the sign characteristics. They first introduced an observer selection strategy based on effective distance to optimize the quality of observers and then proposed a source localization method based on reverse propagation. Although this algorithm takes into account the difference in the propagation ability between positive and negative edges, showing that positive edges usually have a stronger propagation ability, it does not normalize the relationship strength of the same-order neighbors and does not consider the balance issue between positive and negative edges.

The fifth approach is to use graph neural networks for source localization from the perspective of machine learning. Currently, the research on information dissemination in complex networks has gradually shifted from modeling-driven methods to data-driven methods [12–16]. Graph convolutional networks (GCNs) are based on the message-passing mechanism, which realizes the layer-wise propagation of information in the network by iteratively aggregating neighborhood information [17]. Dong et al. [18] were the first to apply GCNs to solve the multisource localization problem, proposing graph convolutional network-based source identification (GCNSI). They took the convergence result of the LPSI algorithm as the model input and considered the situation where positive and negative label values offset each other in label propagation. They aggregated source prominence features from three aspects (the entire graph, only infected nodes, and only uninfected nodes) to achieve multiple rumor source localization. Ling et al. [19] were the first to propose a source localization variational autoencoder (SL-VAE) from a probabilistic perspective, combining the forward diffusion estimation model with the deep generative model to quantify the uncertainty of the source by approximating the distribution of the diffusion source and learning the generation prior to represent the complex patterns of source diffusion with the prior knowledge provided by the observed source-observation pairs. However, VAEs may not sufficiently model the uncertainty of diffusion sources, Xu et al. [20] proposed a probabilistic graph diffusion model for source localization (PGSL), which integrates the deep generative model with the graph neural network (GNN) model. Their PGSL model handles the uncertainty of the diffusion process by normalizing flows and invertible transformations and is empowered with GNNs to capture the information dissemination features, which are able to reconstruct the graph diffusion process under arbitrary diffusion patterns. Yan et al. [21] introduced reversible residual networks and constructed a discrete denoising diffusion model (DDMSL) for restoring diffusion paths and locating diffusion sources. However, this method requires prior knowledge about the propagation model. GNN-based signed graph embedding methods, although specifically designed for signed graphs to learn high-level features and typically utilize multiorder neighbor aggregation and multifaceted attention to fully capture local and global structural features [22,23], mostly fail to learn universal node representations and are only applicable to specific downstream tasks such as link sign prediction and community detection, lacking strong specificity for the multisource rumor localization task. A summary of the comparison of the main literature is presented in Table 1.

Table 1. Comparison table of relevant algorithms.

Year	Name	Network type	Propagation model	Additional information	Algorithm type
2017	LPSI [8]	Unsigned network	General	No	Traditional algorithm
2024	DISLPSI [9]	Signed network	SI	Dynamic selection of observer	Traditional algorithm
2022	BPSL [10]	Unsigned network	SI	Observer selection based on influence maximization	Traditional algorithm
2024	Source localization based on reverse propagation [11]	Signed network	SI	Observer selection based on effective distance	Traditional algorithm
2019	GCNSI [18]	Unsigned network	General	No	Learning algorithm
2022	SL-VAE [19]	Unsigned network	General	Source-observation pairs	Learning algorithm
2024	PGSL [20]	Unsigned network	General	No	Learning algorithm
2023	DDMSL [21]	Unsigned network	SIR	Infection rate and Recovery rate	Learning algorithm
2023	MUSE [22]	Signed network	General	No	Learning algorithm
2024	SiG [23]	Signed network	General	No	Learning algorithm

Due to the fact that social relationships in online social networks often have emotional polarity, such as trust or distrust, friends or enemies, positive attitudes or negative attitudes, users tend to maintain the same opinion with friends and the opposite opinion with enemies, thus forming signed social networks [24]. Moreover, most existing studies ignore the negative edge characteristics and treat them equally with positive edges [25]. Therefore, this paper considers the structural balance properties of signed social networks, sufficiently exploits the different roles of heterogeneous relationships on rumor propagation, and proposes a signed graph convolutional network algorithm combining spatial and spectral domains to specifically address the problem of multirumor source localization in signed social networks. Moreover, the principle of rumor centrality and the theory of source saliency are extended to signed social networks.

The unique advantage of this paper lies in its simultaneous consideration of signed networks and multisource localization, integrating sociological theories with source location features to conduct multisource localization in online social networks. Specifically, compared with the source localization methods in unsigned graphs, this paper takes into account the characteristics of signed social networks, treats positive and negative neighbors differently, and utilizes social psychological theories. Compared with the signed graph embedding methods, this paper utilizes the centrality and salience of sources, making the learned representations more regular. Compared with the methods that require additional information and are applicable to specific propagation models, the algorithm in this paper is more general and practical, only using network snapshots and being applicable to general propagation models.

The main innovations of this paper are as follows:

(1) Based on the theory of structural balance, this paper optimizes the propagation rules and proposes an information propagation model suitable for signed social networks, namely the asymmetric boosting signed susceptible–infected model (AS-SI), to construct the information dissemination process in signed social networks. First, considering the different transmission rates of positive and negative edges, the positive edges are enhanced asymmetrically. Second, it takes into

account the influence of structural balance on the transmission rate, that is, the balanced triangle structure promotes the information dissemination of positive edges and inhibits that of negative edges. Finally, the ultimate AS-SI model based on the SI model is obtained.

(2) This paper leverages the complementary advantages of the rumor centrality principle and the source prominence theory to propose a spatial and spectral domain combined signed graph convolutional network architecture (3SGCN) for addressing the problem of multiple rumor source localization in online social network settings. First, the principle of rumor centrality is generalized to signed networks, and a signed graph convolutional network based on signed attention mechanism is proposed, which implicitly encodes the positional information of nodes in the infection subgraph. Second, the theory of source prominence is generalized to signed networks, and a two-stream graph convolutional network based on label propagation mechanism is proposed to learn the positional distribution features of infected and uninfected nodes. Finally, the multilayer perceptron (MLP) network is used for a binary classification task to detect whether each node is an infection source or not.

The structure of this paper is arranged as follows. Section 2 defines the research problem and constructs the propagation model. Section 3 elaborates on the overall framework of the proposed algorithm, the two main modules it contains, and the objective function that matches the task. Section 4 evaluates the effectiveness of the proposed method through a large number of experiments. Section 5 summarizes the entire paper, points out the limitations of the proposed algorithm, and indicates directions for future development.

2. Problem modeling

2.1. Problem definition

Consider the infected snapshot $G(V, E, S, A)$ of an undirected signed network at a specific time, where V is the node set, E is the edge set, S is the vector formed by the infected states of all nodes, and A is the adjacency matrix. Because this paper regards the MRSL problem as a binary classification task in machine learning, that is, to determine whether each node is a rumor source or not [18], it is defined as finding a classification function $f: V \to \{0,1\}$ such that the set of predicted rumor sources R^* satisfies Eq (2.1), where $f(v_i) = 0$ indicates that v_i is not rumor source; otherwise, $f(v_i) = 1$ indicates it is rumor source, R is the set of true rumor sources, and $R^* = \{v_i \in V | f(v_i) = 1\}$.

$$R^* = \underset{R}{argmax} \frac{|R^* \cap R|}{|R^* \cup R|}. \tag{2.1}$$

It should be noted that, considering the bidirectional characteristics of rumor propagation and diffusion [26], this paper mainly studies the information dissemination patterns and source localization strategies in undirected signed networks. The mathematical notations of this paper are summarized in Table 2.

Table 2. Mathematical notations.

Notation	Description
v_i	The node i.
$e_{i,j}$	The edge between v_i and v_j.
s_i	The infection state of v_i, each $s_i \in \{-1,1\}$, where $s_i = -1$ means that v_i is uninfected, and otherwise $s_i = 1$ means it is infected.
a_{ij}	The sign of e_{ij}, each $a_{ij} \in \{-1,0,1\}$, where $a_{ij} = -1$ means that e_{ij} is a negative edge, $a_{ij} = 1$ means that e_{ij} is a positive edge, and $a_{ij} = 0$ means that there exists no edge between v_i and v_j.
$G(V,E,S,A)$	The infected snapshot of an undirected signed network at a given time, where V is the node set, E is the edge set, S is the vector composed of the infected states of all nodes, A is the adjacency matrix, s_i is an element of S, and a_{ij} is an element of A.
$G_1(V,E_1,S,A_1)$	The subgraph formed by all nodes and their positive edges in G, where E_1 is the edge set of G_1, A_1 is the adjacency matrix of G_1, and its elements take values from the set $\{0,1\}$, where 0 indicates no edge exists, and 1 indicates an edge exists.
$G_2(V,E_2,S,A_2)$	The subgraph formed by all nodes and their negative edges in G, where E_2 is the edge set of G_2, A_2 is the adjacency matrix of G_2, and its elements take values from the set $\{0,1\}$, where 0 indicates no edge exists, and 1 indicates an edge exists.
D_1	The degree matrix of A_1, which is a diagonal matrix with its (i,i)-element equal to the sum of the i-th row of A_1.
D_2	The degree matrix of A_2.
λ	The asymmetric boosting coefficient, $\lambda > 1$.
γ	The constant infection probability, $0 < \gamma < 1$.
$\mu_{i,j}^{+}$	The positive edge transmission rate.
$\mu_{i,j}^{-}$	The negative edge transmission rate.
$\beta_{i,j}^{+}$	The positive edge infection intensity.
$\beta_{i,j}^{-}$	The negative edge infection intensity.
$\alpha_{i,j}^{+}$	The positive edge attention weight.
$\alpha_{i,j}^{-}$	The negative edge attention weight.
N_i	The set of v_i's direct linked neighbors.
N_i^{+}	The set of v_i's neighbors linked by a positive edge.
N_i^{-}	The set of v_i's neighbors linked by a negative edge.
$N_{i,l}$	The set of l-order neighbors of v_i, where $N_{i,1} = N_i$.
$N_{i,l}^{+}$	The set of l-order neighbors of v_i connected with $(l-1)$-order neighbors by a positive edge, where $N_{i,1}^{+} = N_i^{+}$.
$N_{i,l}^{-}$	The set of l-order neighbors of v_i connected with $(l-1)$-order neighbors by a negative edge, where $N_{i,1}^{-} = N_i^{-}$.
$B_i(l)$	The set of l-order positive neighbors that v_i reaches through a balanced path of length l.
$U_i(l)$	The set of l-order negative neighbors that v_i reaches through an unbalanced path of length l.
$H_1^{(l)}$	The result of performing l-layer spectral domain GCN on G_1.
$H_2^{(l)}$	The result of performing l-layer spectral domain GCN on G_2.
H	The final output of the spatial GCN module, where the element of H is denoted as h_i.
H'	The final output of the spectral GCN module, where the element of H' is denoted as h_i'.
h_i	The final position embedding of v_i, namely the feature representation of rumor centrality.
h_i'	The final label value of v_i, namely the feature representation of source prominence.
L_1	The number of convolutional layers in the spatial GCN module.
L_2	The number of convolutional layers in the spectral GCN module.

2.2. Propagation model

According to the characteristics of rumor spreading in online social networks, based on the structural balance theory of social psychology, combining the complementary advantages of the S-SI and MFC models, this paper proposes an asymmetric boosting signed susceptible–infected (AS-SI) model. First, inspired by the S-SI propagation model [7], in accordance with the structural balance theory and considering the balance of triangular structure, a balanced triangular relationship facilitates the dissemination of the same information, and an unbalanced one promotes the propagation of opposite information. Thus, the transmission rate of a positive or negative edge is defined as the proportion of balanced or unbalanced triangles, respectively, in which it is involved. Second, inspired by the MFC propagation model [6], considering the different effects of heterogeneous relationships on the transmission rates, the asymmetric boosting coefficient λ is introduced to improve the transmission rate of positive edges. Finally, the AS-SI model of this paper is obtained by optimizing the SI model. The specific calculation process is as follows:

In accordance with the structural balance theory in social psychology [27,28], taking into account the balance of triangular structures and that of propagation paths, balanced triangles and unbalanced triangles, as well as balanced paths and unbalanced paths, are defined respectively, as shown in Figure 1. The number of negative edges in balanced triangles and balanced paths is even, while in unbalanced triangles and unbalanced paths, it is odd.

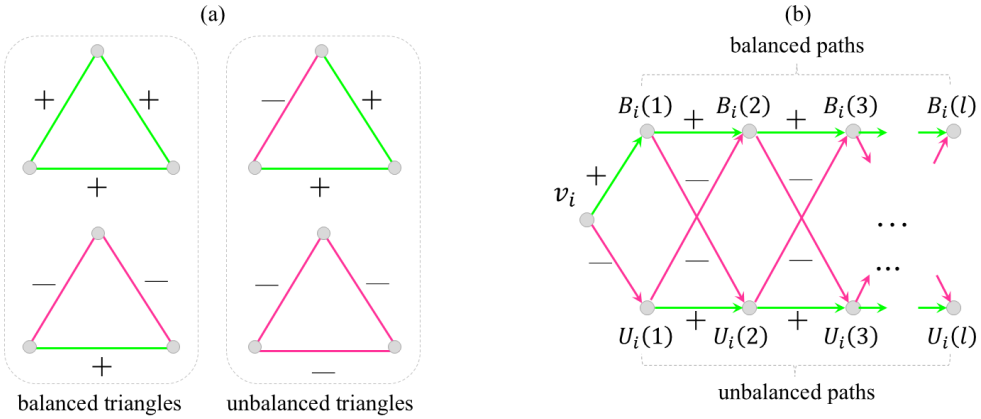

Figure 1. The structural balance theory. (a) The balance of triangular structures; (b) The balance of propagation paths.

(1) According to the balance of triangles, the transmission rate and infection intensity of positive/negative edges are defined.

First, based on the structural balance theory, the transmission rate of a positive/negative edge is calculated. If the edge $e_{i,j}$ constitutes a triangular structure with other edges in the network, when $a_{ij} = 1$, the $e_{i,j}$'s transmission rate $\mu_{i,j}^{+}$ is presented in Eq (2.2); when $a_{ij} = -1$, the $e_{i,j}$'s transmission rate $\mu_{i,j}^{-}$ is presented in Eq (2.3). If the edge $e_{i,j}$ does not form a triangular structure with any edge, when $a_{ij} = 1$, the $e_{i,j}$'s transmission rate is $\mu_{i,j}^{+} = 1$, and when $a_{ij} = -1$, the $e_{i,j}$'s transmission rate is $\mu_{i,j}^{-} = 0$.

$$\mu_{i,j}^{+}=\frac{\sum_{k\in N_i\cap N_j} max\left\{0,a_{ij}\times a_{ik}\times a_{jk}\right\}}{\sum_{k\in N_i\cap N_j}\left|a_{ij}\times a_{ik}\times a_{jk}\right|}, \tag{2.2}$$

$$\mu_{i,j}^{-}=\frac{\left|\sum_{k\in N_i\cap N_j} min\left\{0,a_{ij}\times a_{ik}\times a_{jk}\right\}\right|}{\sum_{k\in N_i\cap N_j}\left|a_{ij}\times a_{ik}\times a_{jk}\right|}, \tag{2.3}$$

where v_i, v_j, v_k denote the vertices of the triangle, and $\left|N_i\cap N_j\right|$ denotes the total number of triangles that contain the edge $e_{i,j}$.

Second, based on the AS-SI model proposed in this paper, the infection intensity of the positive/negative edge is computed. When $a_{ij}=1$, the infection intensity $\beta_{k,j}^{+}$ of $e_{i,j}$ is shown in Eq (2.4). When $a_{ij}=-1$, the infection intensity $\beta_{k,j}^{-}$ of $e_{i,j}$ is shown in Eq (2.5).

$$\beta_{k,j}^{+}=\lambda\times\gamma\times\mu_{i,j}^{+}, \tag{2.4}$$

$$\beta_{k,j}^{-}=\gamma\times\mu_{i,j}^{-}, \tag{2.5}$$

where λ denotes the asymmetric boosting coefficient, and γ denotes the constant infection probability.

(2) According to the balance of the path, the set of positive/negative neighbors is defined recursively.

Based on the structural balance theory, the positive neighbors on the balanced path are regarded as friends, and the negative neighbors on the unbalanced path are regarded as enemies. When $l=1$, the *1*-order positive neighbors set $B_i(1)$ and the *1*-order negative neighbors set $U_i(1)$ of v_i are expressed in Eqs (2.6) and (2.7), respectively. When $l>1$, the set of l-order positive neighbors $B_i(l)$ and the set of l-order negative neighbors $U_i(l)$ of v_i are expressed in Eqs (2.8) and (2.9), respectively:

$$B_i(1)=N_i^{+}=\left\{v_j|v_j\in N_i^{+}\right\}, \tag{2.6}$$

$$U_i(1)=N_i^{-}=\left\{v_j|v_j\in N_i^{-}\right\}, \tag{2.7}$$

$$B_i(l)=\left\{v_j|v_k\in B_i(l-1)\wedge v_j\in N_k^{+}\right\}\cup\left\{v_j|v_k\in U_i(l-1)\wedge v_j\in N_k^{-}\right\}, \tag{2.8}$$

$$U_i(l)=\left\{v_j|v_k\in U_i(l-1)\wedge v_j\in N_k^{+}\right\}\cup\left\{v_j|v_k\in B_i(l-1)\wedge v_j\in N_k^{-}\right\}. \tag{2.9}$$

The following provides an example for illustration. As shown in Figure 2(a), suppose edge $e_{1,2}$ forms only three triangular structures in the network, namely $v_1v_2v_3$, $v_1v_2v_4$, and $v_1v_2v_5$. For the first two triangles, because there are an even number of negative edges, they are balanced triangles. The last triangle, however, is an unbalanced triangle due to the odd number of negative edges. As edge $e_{1,2}$ is a positive edge, its propagation rate is the proportion of balanced triangles, that is, $\mu_{1,2}^{+}=\frac{2}{3}$. As shown in Figure 2(b), if the current node is v_1, then v_2 and v_3 are its third-order positive and negative neighbors, respectively. This is because the path from v_1 to v_2 contains an even number of negative edges, making it a balanced path. Conversely, the path from v_1 to v_3 is an unbalanced path.

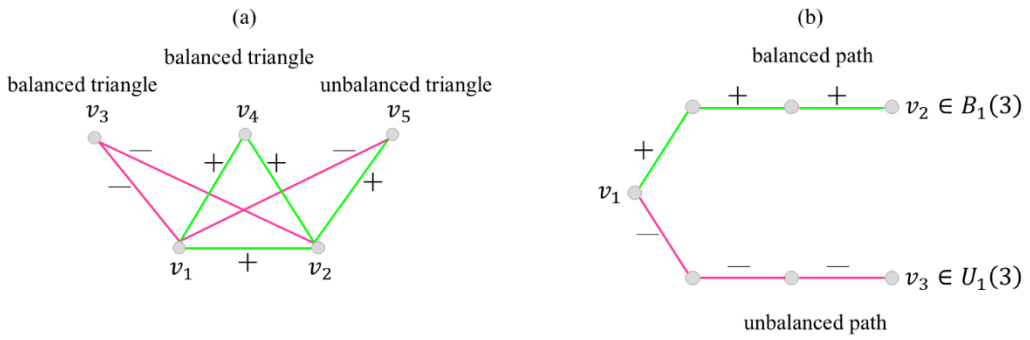

Figure 2. Simple example. (a) Calculate the propagation rate of the edge; (b) Determine positive and negative neighbors.

3. General framework

In this paper, by integrating the complementary advantages of model-driven and data-driven approaches, a new architecture of signed graph convolutional networks combining spatial and spectral domains (3SGCN) is proposed for multisource rumor localization in online social networks. First, according to the characteristics of rumor propagation in signed social networks, an AS-SI model based on structural balance theory and asymmetric enhancement is proposed to describe the distinct contributions of positive and negative edges in information dissemination. Second, the original network snapshot is divided into the subgraph consisting of only infected nodes and their edges, the subgraph consisting of only positive edges and the subgraph consisting of only negative edges, and the propagation structure features are extracted from different perspectives to encode the positional information of nodes. Finally, the principle of rumor centrality and the theory of source prominence are generalized to the signed network, establishing the coherent logic between qualitative theoretical models and quantitative learning algorithms, comprehensively extracting the propagation structural features and learning the positional representation from big data, thereby improving the accuracy and robustness of the multisource rumor localization task in the specific context of signed social networks. The overall framework of the proposed 3SGCN is shown in Figure 3, mainly including graph preprocessing, the spatial domain GCN module, the spectral domain GCN module, and the MLP classifier.

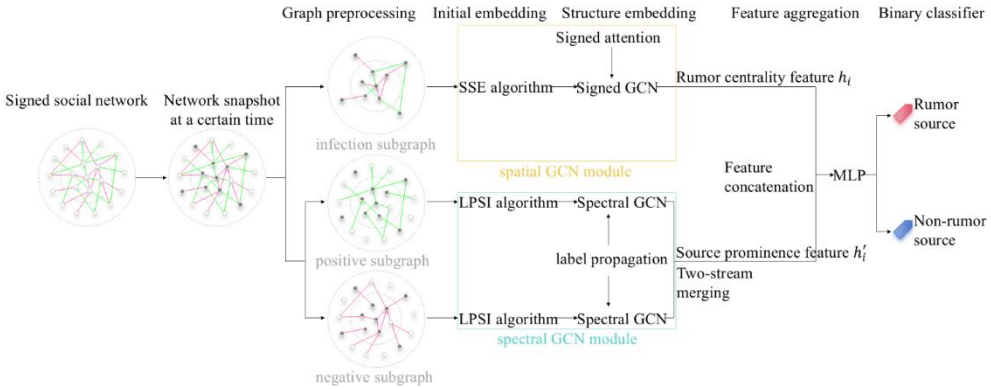

Figure 3. The overall framework of 3SGCN mainly consists of four modules, namely graph preprocessing, spatial domain GCN module, spectral domain GCN module, and MLP classifier.

The first module is graph preprocessing, which splits the network snapshot into different subgraphs, namely the infection subgraph, the positive-only subgraph, and the negative-only subgraph. In the spatial GCN module, the initial embedding is first obtained by applying the signed spectral embedding (SSE) algorithm based on signed spectral clustering. Then, the signed graph convolutional network based on the signed attention mechanism proposed in this paper is utilized to extract the propagation structure features of the infected nodes. The characteristics of this module are that it considers the underlying propagation model and the interrelationship between positive and negative edges, learns the position information of the source nodes from the mixed path, and generalizes the principle of rumor centrality to signed social networks. In the spectral GCN module, the initial embedding is first obtained by utilizing the LPSI algorithm based on label propagation, and then the two-stream graph convolutional network based on the label propagation mechanism proposed in this paper is employed to extract the position distribution features of the infected nodes and the uninfected nodes. This module does not rely on the underlying propagation model and treats positive and negative edges differently, learning the position information of the source nodes from the single path and generalizing the source significance theory to the signed social network. The last module is the MLP classifier. In this paper, the MRSL problem is transformed into a binary classification problem for all nodes, and the MLP is used to output whether each node is a rumor source or not.

3.1. Spatial GCN module

In accordance with the principle of rumor centrality, the likelihood that node v_i being the source node in the infection subgraph is proportional to the weighted sum of the number of distinct spreading orders starting from this node, where the weight of a spreading order could depend on the specific graph structure and spreading time distribution of the SI model. In other words, the source node tends to be in the center position of the network structure, and its paths to all nodes could be as many and as close as possible. Hence, this paper extends to signed social networks, encodes all the reachable paths of nodes from balanced and unbalanced paths respectively, and employs the normalized positive and negative infection intensities as signed attention weights, proposing a signed graph convolutional network based on a signed attention mechanism to learn the source centrality representation of nodes by extracting the propagation structure features of infected nodes. It is worth noting that for the embedding representation of uninfected nodes, this paper sets them as zero vectors of the same dimension. The details of this module are as follows:

(1) The initial position embedding of the infected nodes is obtained by employing the SSE algorithm [29], and the l-order positively linked neighbor set $N_{i,l}^{+}$ and the l-order negatively linked neighbor set $N_{i,l}^{-}$ of the infected node v_i are recursively defined. When $l = 1$, $N_{i,1}^{+}$ and $N_{i,1}^{-}$ are presented by Eqs (3.1) and (3.2); when $l > 1$, $N_{i,l}^{+}$ and $N_{i,l}^{-}$ are depicted in Eqs (3.3) and (3.4).

$$N_{i,1}^{+} = N_i^{+} = \{v_j | v_j \in N_i^{+}\}, \tag{3.1}$$

$$N_{i,1}^{-} = N_i^{-} = \{v_j | v_j \in N_i^{-}\}, \tag{3.2}$$

$$N_{i,l}^{+} = \{v_j | v_k \in B_i(l-1) \wedge v_j \in N_k^{+}\} \cup \{v_j | v_k \in U_i(l-1) \wedge v_j \in N_k^{+}\}, \tag{3.3}$$

$$N_{i,l}^{-} = \{v_j | v_k \in B_i(l-1) \wedge v_j \in N_k^{-}\} \cup \{v_j | v_k \in U_i(l-1) \wedge v_j \in N_k^{-}\}, \tag{3.4}$$

where the v_i's l-order neighbor set $N_{i,l} = N_{i,l}^{+} \cup N_{i,l}^{-} = B_i(l) \cup U_i(l)$, $B_i(l)$ represents the l-order positive neighbor set of v_i, and $U_i(l)$ represents the l-order negative neighbor set of v_i.

(2) Inspired by the signed attention networks [30,31] but considering the differences in the

propagation model and learning tasks, this paper proposes a calculation method for positive/negative attention weights to measure the trust degree between social users.

Let the v_i's $(l-1)$-order neighbor be v_k and l-order neighbor be v_j. When $a_{kj}=1$, the $e_{k,j}$'s positive attention weight is $\alpha^{+}_{k,j}$ as shown in Eq (3.5); when $a_{kj}=-1$, the $e_{k,j}$'s negative attention weight is $\alpha^{-}_{k,j}$ as shown in Eq (3.6).

$$\alpha^{+}_{k,j}=\frac{\beta^{+}_{k,j}}{|N^{+}_{i,l}|}, \tag{3.5}$$

$$\alpha^{-}_{k,j}=\frac{\beta^{-}_{k,j}}{|N^{-}_{i,l}|}, \tag{3.6}$$

where $\beta^{+}_{k,j}$ indicates the positive infection intensity of $e_{k,j}$, $\beta^{-}_{k,j}$ indicates the negative infection intensity of $e_{k,j}$, and $|\cdot|$ indicates the modulus of a set.

(3) Inspired by signed graph convolutional networks (SGCN) [32], in order to align with the multirumor source localization task in signed social networks, this paper proposes a signed graph convolutional network based on the signed attention mechanism. It performs neighborhood aggregation from balanced and unbalanced paths, respectively, and assigns distinct attention weights to positive and negative neighbors. Eventually, the high-order friend and enemy representations of nodes are obtained. The specific process is depicted in Figure 4.

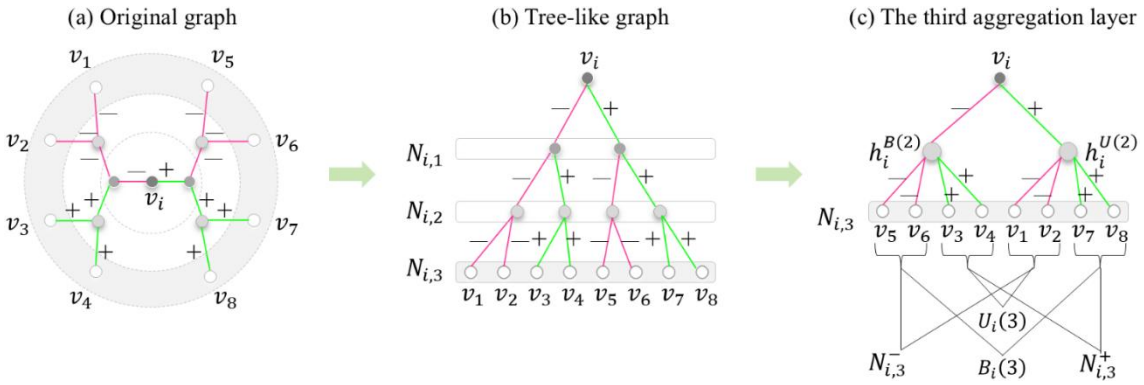

Figure 4. A simple network with eight nodes for illustrating the aggregation process in spatial GCN module. (a) represents the given original graph. (b) denotes the tree-like graph derived from the original graph. (c) illustrates the graph structure during the aggregation of the third layer.

Let the v_i's initial embedding representation be $h_i^{(0)}$, and after each layer of aggregation, two representations of v_i can be obtained, namely the friend and enemy representations.

First, after the first aggregation layer, the *1*-order friend representation $h_i^{B(1)}$ and the *1*-order enemy representation $h_i^{U(1)}$ of v_i are obtained, as expressed in Eqs (3.7) and (3.8).

$$h_i^{B(1)}=\sigma\left(W^{B(1)}\left[\sum_{v_j\in B_i(1)}\ \alpha^{+}_{i,j}\times h_j^{(0)},h_i^{(0)}\right]\right), \tag{3.7}$$

$$h_i^{U(1)}=\sigma\left(W^{U(1)}\left[\sum_{v_j\in U_i(1)}\ \alpha^{-}_{i,j}\times h_j^{(0)},h_i^{(0)}\right]\right), \tag{3.8}$$

where $h_i^{(0)}$ and $h_j^{(0)}$ respectively denote the initial embedding representations of v_i and v_j, $W^{B(1)}$ and $W^{U(1)}$ are the weight matrices to be learned, and σ denotes the activation function.

Second, after the l-layer $(l \geq 2)$ of aggregation, the l-order friend representation $h_i^{B(l)}$ and the l-order enemy representation $h_i^{U(l)}$ of v_i are presented in Eqs (3.9) and (3.10).

$$h_i^{B(l)} = \sigma\left(W^{B(l)}\left[\sum_{\substack{v_k \in B_i(l-1) \\ v_j \in B_i(l)}} \alpha_{k,j}^{+} \times h_j^{B(l-1)}, \sum_{\substack{v_k \in U_i(l-1) \\ v_j \in B_i(l)}} \alpha_{k,j}^{-} \times h_j^{U(l-1)}, h_i^{B(l-1)}\right]\right), \tag{3.9}$$

$$h_i^{U(l)} = \sigma\left(W^{U(l)}\left[\sum_{\substack{v_k \in U_i(l-1) \\ v_j \in U_i(l)}} \alpha_{k,j}^{+} \times h_j^{U(l-1)}, \sum_{\substack{v_k \in B_i(l-1) \\ v_j \in U_i(l)}} \alpha_{k,j}^{-} \times h_j^{B(l-1)}, h_i^{U(l-1)}\right]\right), \tag{3.10}$$

where $\alpha_{k,j}^{+}$ represents the positive attention weight of $e_{k,j}$, $\alpha_{k,j}^{-}$ represents the negative attention weight of $e_{k,j}$, $W^{B(l)}$ and $W^{U(l)}$ represent the weight matrices to be learned, and σ represents the activation function.

It is worth noting that the l-order friend representation $h_i^{B(l)}$ of v_i aggregates neighbor information from two aspects, namely the neighbors of its $(l-1)$-order friend connected through a positive edge and the neighbors of its $(l-1)$-order enemy connected through a negative edge. Similarly, the l-order enemy representation $h_i^{U(l)}$ of v_i also aggregates neighbor information from two aspects, namely the neighbors of its $(l-1)$-order enemy connected through a positive edge and the neighbors of its $(l-1)$-order friend connected through a negative edge.

Finally, after the L_1-layer $(L_1 \geq 2)$ of aggregation, the two hidden representations $H^{B(L_1)}$ and $H^{U(L_1)}$ are concatenated to obtain the final embedded representation H of all infected nodes, as shown in Eq (3.11).

$$H = concat\left(H^{B(L_1)}, H^{U(L_1)}\right), \tag{3.11}$$

where $H^{B(L_1)} = \left[h_1^{B(L_1)}, h_2^{B(L_1)}, \cdots, h_{|V|}^{B(L_1)}\right]^T$, $H^{U(L_1)} = \left[h_1^{U(L_1)}, h_2^{U(L_1)}, \cdots, h_{|V|}^{U(L_1)}\right]^T$ and $concat(\cdot)$ represents the concatenation operation.

3.2. Spectral GCN module

The spatial GCN module focuses on the propagation structure characteristics of infected nodes under the AS-SI model, learns the source centrality representation of nodes, and captures the interaction of heterogeneous edges in the propagation structure by encoding the mixed path composed of positive and negative edges. The spectral GCN module, however, focuses on the positional distribution characteristics of infected and uninfected nodes without relying on the underlying diffusion model, learns the source prominence representation of nodes, and encodes the single paths constituted by positive and negative edges, respectively, to capture the different impacts of heterogeneous edges on the dissemination structure. Hence, the spatial GCN module and the spectral GCN module are complementary to each other and integrate qualitative theoretical models with quantitative data learning to describe the positional information of rumor sources comprehensively and from multiple perspectives, thereby enhancing the accuracy and robustness of the multirumor source localization. This not only validates the rumor centrality principle and the source prominence theory but also extends them to signed social networks. In the spectral GCN module, inspired by the LPSI algorithm [8] and its variants [18], this paper transforms the MRSL problem into a label

propagation problem and subsequently into a binary classification problem. Meanwhile, the convergence result of label propagation is utilized as input to improve the training efficiency and learning quality of the model. Second, the idea of subgraph splitting in the relational graph neural networks [33] is combined with the two-stream graph convolutional networks architecture [34]. Simultaneously taking into account the inherent inconsistency of the propagation structure constituted by positive and negative edges, the original network snapshot is decomposed into a subgraph containing only positive edges and a subgraph containing only negative edges, and two-stream spectral domain graph convolution operations are performed on these two subgraphs. Finally, the two label values are aggregated with weights to obtain the source prominence representation of all nodes.

According to the source prominence theory, the proportion of infected nodes surrounding the source node is typically higher. In other words, the nodes surrounded by larger proportions of infected nodes are more likely to be infection sources [8]. Hence, the positional distribution of infected and uninfected nodes can be utilized for source localization. The source localization method based on label propagation applies the source prominence theory to label propagation. Initially, it considers the scenario of two types of labels competing to propagate in the network, where the positive labels of infected nodes and the negative labels of uninfected nodes are simultaneously propagated. The source node, as the "strongest" infected node, often has the maximum label value in its local neighborhood. Nevertheless, due to the mutual cancellation of positive and negative labels, the scenario of single-label propagation is considered, concerning only the propagation of positive labels by infected nodes and only the propagation of negative labels by uninfected nodes. Nodes with the local maximum positive label value and the local minimum negative label value are frequently the source nodes. On this basis, this paper takes into account the different propagation structures formed by heterogeneous edges in signed networks. First, the original graph is split into positive-only and negative-only subgraphs. Then, the label distribution features are respectively extracted from the two subgraphs. The positive and negative label values, positive label values, and negative label values of each node are iteratively calculated, corresponding separately to the three situations of competitive propagation: positive and negative labels, only positive labels, and only negative labels. It should be noted that in this paper, the label convergence result is adopted as the initial label value, and the spectral domain graph convolution operation [35] is used to realize the label propagation process. The main steps of this module are as follows:

(1) Based on the convergence result of label propagation [8], the initial embeddings $H_1^{(0)}$ and $H_2^{(0)}$ of the positive subgraph G_1 and the negative subgraph G_2 are generated. The specific process is shown in Algorithm 1. In lines 4–10 of Algorithm 1, S_1 is a vector generated by changing all -1 to 0 in S, and S_2 is a vector generated by changing all 1 to 0 in S. S, S_1, and S_2 respectively represent the initial label values of all nodes in the three scenarios of positive and negative label competitive propagation, only positive label propagation, and only negative label propagation. As introduced in lines 11–13, $H_1^{(0)}$ consists of three components, $H_{11}^{(0)}$, $H_{12}^{(0)}$ and $H_{13}^{(0)}$, which respectively represent the final label values of all nodes obtained by applying the label convergence formula to graph G_1 under the three propagation scenarios S, S_1, and S_2. As presented in lines 14–16, $H_2^{(0)}$ consists of three components, $H_{21}^{(0)}$, $H_{22}^{(0)}$ and $H_{23}^{(0)}$, which respectively represent the final label values of all nodes in the three propagation scenarios obtained by applying the label convergence formula to S, S_1, and S_2 in G_2.

Algorithm 1. Input Generation

Input: The positive-only networks $G_1(V, E_1, S, A_1)$ and the negative-only networks $G_2(V, E_2, S, A_2)$ based on the infected networks $G(V, E, S, A)$,where $S = (s_1, s_2, \cdots, s_{|V|})^T$; parameter φ;

1. Initial label value matrices $H_1^{(0)} = \left[H_{11}^{(0)}, H_{12}^{(0)}, H_{13}^{(0)}\right], H_2^{(0)} = \left[H_{21}^{(0)}, H_{22}^{(0)}, H_{23}^{(0)}\right]$;
2. Construct the matrices $M_1 = {D_1}^{-\frac{1}{2}} \times A_1 \times {D_1}^{-\frac{1}{2}}$ and $M_2 = {D_2}^{-\frac{1}{2}} \times A_2 \times {D_2}^{-\frac{1}{2}}$, where D_1 and D_2 are the diagonal matrices with their (i, i)-element equal to the sum of the i-th row of A_1 and A_2, separately;
3. Initialize the vectors $S_1 = S_2 = S$ where $S_1 = (s_{11}, s_{12}, \cdots, s_{1|V|})^T, S_2 = (s_{21}, s_{22}, \cdots, s_{2|V|})^T$;
4. **for** $i < len(S)$ **do**
5. **if** $s_i == -1$ **then**
6. $s_{1i} = 0$;
7. **else**
8. $s_{2i} = 0$;
9. **end if**
10. **end for**
11. $H_{11}^{(0)} = (1 - \varphi) \times (I - \varphi M_1)^{-1} \times S$;
12. $H_{12}^{(0)} = (1 - \varphi) \times (I - \varphi M_1)^{-1} \times S_1$;
13. $H_{13}^{(0)} = (1 - \varphi) \times (I - \varphi M_1)^{-1} \times S_2$;
14. $H_{21}^{(0)} = (1 - \varphi) \times (I - \varphi M_2)^{-1} \times S$;
15. $H_{22}^{(0)} = (1 - \varphi) \times (I - \varphi M_2)^{-1} \times S_1$;
16. $H_{23}^{(0)} = (1 - \varphi) \times (I - \varphi M_2)^{-1} \times S_2$;
17. **return** $H_1^{(0)} = concat\left(H_{11}^{(0)}, H_{12}^{(0)}, H_{13}^{(0)}\right), H_2^{(0)} = concat\left(H_{21}^{(0)}, H_{22}^{(0)}, H_{23}^{(0)}\right)$;

(2) Spectral domain GCN is performed on G_1 and G_2, respectively, and the graph convolution operations for each layer are shown in Eqs (3.12) and (3.13).

$$H_1^{(l)} = \sigma\left(\widetilde{M_1} H_1^{(l-1)} W_1^{(l-1)}\right), \tag{3.12}$$

$$H_2^{(l)} = \sigma\left(\widetilde{M_2} H_2^{(l-1)} W_2^{(l-1)}\right), \tag{3.13}$$

where $H_1^{(l)}$ and $H_2^{(l)}$ respectively denote the outcomes of applying the l-layer spectral domain GCN to G_1 and G_2; $\widetilde{M_1}$ and $\widetilde{M_2}$ denote the convolution kernel functions; $\widetilde{M_1} = \widetilde{D_1}^{-\frac{1}{2}} \times \widetilde{A_1} \times \widetilde{D_1}^{-\frac{1}{2}}$, $\widetilde{M_2} = \widetilde{D_2}^{-\frac{1}{2}} \times \widetilde{A_2} \times \widetilde{D_2}^{-\frac{1}{2}}$, $\widetilde{A_1} = A_1 + I$, $\widetilde{A_2} = A_2 + I$, A_1, and A_2 denote the adjacency matrices of G_1 and G_2; I is the identity matrix; $\widetilde{D_1}$ and $\widetilde{D_2}$ denote the degree matrices of $\widetilde{A_1}$ and $\widetilde{A_2}$; $W_1^{(l-1)}$ and $W_2^{(l-1)}$ are the weight matrices to be learned; and σ denotes the activation function.

(3) By stacking L_2-layer spectral domain graph convolution and merging the outputs of two parallel networks together with weight, the final label value of all nodes is acquired as shown in Eq (3.14).

$$H' = \delta H_1^{(L_2)} + (1 - \delta) H_2^{(L_2)}, \tag{3.14}$$

where δ is the adjustment weight.

3.3. Classifier

The final module in the proposed model is the classifier. First, we synthesize the output of the

spatial GCN module and the spectral GCN module into a concatenated representation as the ultimate position of all nodes as presented in Eq (3.15). Subsequently, the MLP classifier is employed to undertake a binary classification task, distinguishing whether each node is a rumor source or not. The MLP classifier is depicted in Eq (3.16), and the cross-entropy loss function is given in Eq (3.17).

$$X = concat(H, H^{'}), \tag{3.15}$$

$$\hat{Y} = sigmoid\big(MLP(X)\big), \tag{3.16}$$

$$loss = -\sum_{v_k \in V} \quad (y_k \times log\, \widehat{y_k} + (1 - y_k) \times log(1 - \widehat{y_k})), \tag{3.17}$$

where H represents the source centrality feature matrix; H' represents the source prominence feature matrix; $concat(\cdot)$ indicates the concatenation operation; $\hat{Y} = \left[\widehat{y_1}, \cdots, \widehat{y_{|V|}}\right]^T$, $\widehat{y_k}$ denotes the predicted label; and y_k denotes the true label.

The 3SGCN algorithm mainly consists of two parts: spatial GCN and spectral GCN, with corresponding time complexities of $O(|V|^2 * L_1)$ and $O(|V|^3 * L_2)$, respectively. Therefore, the overall time complexity of this algorithm is $O(|V|^3 * L_2)$.

4. Experiment and discussion

This paper proposes a multirumor source localization framework tailored to signed social networks. First, an AS-SI propagation model based on the structural balance theory is put forward, which accurately depicts the distinct impacts of positive and negative relationships on message passing in signed networks. Second, a multirumor source localization approach called 3SGCN is proposed, which integrates the rumor centrality principle and the source prominence theory. It thoroughly excavates the propagation structure information of infected nodes as well as the positional distribution information between infected and uninfected nodes. By encoding the source centrality and source prominence features of nodes, the task of multirumor source localization is achieved.

To verify the effectiveness of the algorithm presented in this paper, four real-world online social network datasets are chosen, namely Bitcoin-Alpha [36], Bitcoin-OTC [36], Slashdot [37], and Epinions [37]. The statistics of these datasets are showed in Table 3. Bitcoin-Alpha and Bitcoin-OTC are weighted and directed signed networks composed of Bitcoin transaction users and their trust relationship scores. Its edge weights range from -10 (complete distrust) to +10 (complete trust), with a step of 1, representing various emotional relationships from complete distrust to complete trust. Slashdot is a directed signed network composed of news comment users and their marked friend or enemy relationships. Epinions is a directed signed network composed of product review users and their support or opposition relationships.

Table 3. The statistics of four signed social networks. 'nodes' depicts the number of nodes, 'pos edges' indicates the number of positive edges, 'neg edges' shows the number of negative edges, and '%pos' presents the proportion of positive edges within the network.

networks	nodes	pos edges	neg edges	%pos
Bitcoin-Alpha	3783	22650	1536	93.65
Bitcoin-OTC	5881	32029	3563	89.99
Slashdot	82140	425072	124130	77.40
Epinions	131828	717667	123705	85.30

In order to serve the task of multiple rumor source localization, this paper utilizes the directional information in the graph to construct diffusion cascades. Specifically, for Bitcoin-Alpha and Bitcoin-OTC, Bitcoin users are considered as infection sources, and their transaction counterparts are regarded as infection nodes; for Slashdot and Epinions, comment users are considered as infection sources, and their follow-up commenters are regarded as infection nodes. The construction process of the infection source set is to add users randomly one by one until the number of infected nodes in the network reaches the specified value and then stops.

4.1. Experimental settings

The experimental environment of this paper is equipped with an Intel (R) Core (TM) i9-14900HX CPU and an NVIDIA GeForce RTX 4090 24GB GPU. Pytorch [38] and Pytorch Geometric [39] are utilized. Hyperparameters are adjusted for different datasets. The range of GCN layers is {4, 6, 8, 10}, the range of hidden layer dimensions is {64, 128, 256, 512}, the range of dropout rates is {0.2, 0.3, 0.4, 0.5}, the range of learning rates is {0.001, 0.003, 0.005}, and the range of training epochs is {1000, 1500, 2000}. Five-fold cross-validation is adopted. The original dataset is randomly partitioned into a training set and a test set at a ratio of 4:1. Subsequently, the training set is further divided into a new training set and a validation set in the same ratio. As a result, the proportion of the training set, validation set and test set is 16:4:5. Here, the training set is utilized for learning the model parameters, the validation set is employed to optimize the hyperparameters, and the test set is used to assess the performance of the algorithm. The rectified linear unit (ReLU) function is selected as the activation function in GCN, and the number of hidden layers in MLP is set to 2. The model is trained using the Adam optimization algorithm and the Dropout strategy, and early stopping is implemented. Training will be terminated in advance when the loss function of the validation set shows no decrease over 10 consecutive training rounds. Following the LPSI algorithm, the parameter φ is set to 0.5. Referring to the MFC model, the parameter λ is set to 3. All evaluation metrics are the average of 500 independent experiments to ensure the credibility of the results.

Considering an imbalance between the number of positive and negative samples, this paper selects the F1-score and AUC (i.e., the area under the receiver operating characteristic (ROC) curve) as evaluation metrics. Generally speaking, higher F1 and AUC mean better performance. It can be proved that maximizing the F1-score is equivalent to maximizing Eq (2.1) [18].

4.2. Comparison results

To verify the superiority of the 3SGCN algorithm proposed in this paper, six state-of-the-art baseline models are selected for performance comparison: LPSI [8], GCNSI [18], SL-VAE [19], PGSL [20], multifaceted attention-based signed network embedding (MUSE) [22], and global information-based signed network embedding (SiG) [23], which are described as follows. The hyperparameters of the above models are chosen according to their original papers. In this paper, the proportion of infected nodes is set to range from 10% to 20%, and extensive experiments are conducted on four real-world social network datasets. Then, the changing trends of the F1-score and AUC of each model is obtained, as depicted in Figure 5.

- LPSI: A multisource detection framework based on label propagation.
- GCNSI: A multirumor source detection framework based on graph convolutional networks.
- SL-VAE: A multisource localization framework based on variational autoencoder.
- PGSL: A multisource localization framework combining deep generative and graph neural

network models.

- MUSE: A signed network embedding method based on multifaceted attention mechanism.
- SiG: A signed network embedding method based on global information.

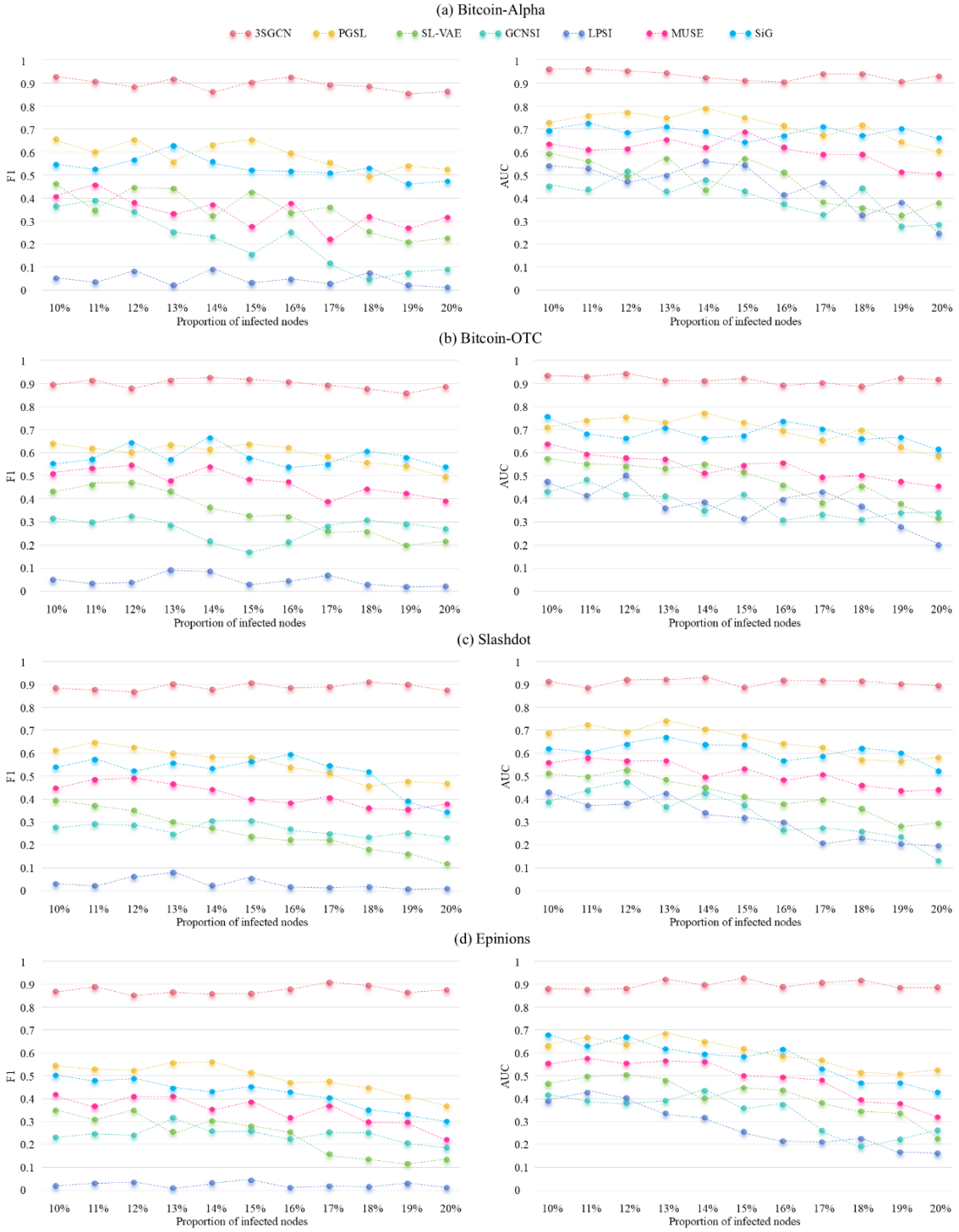

Figure 5. The performance comparison of five algorithms on four datasets. The subgraphs depict the variations in the F1-scores and AUC values of all algorithms as the percentage of infected nodes ranges from 10% to 20% in the following datasets: (a) Bitcoin-Alpha, (b) Bitcoin-OTC, (c) Slashdot, and (d) Epinions. Distinct curves correspond to different algorithms.

The paired t-test results of the algorithm in this paper are shown in Table 4. Statistical significance: ***, **, * for p-value<0.01, 0.05, 0.1 respectively.

Table 4. Statistical significance of 3SGCN.

	Bitcoin-Alpha		Bitcoin-OTC		Slashdot		Epinions	
3SGCN	F1	AUC	F1	AUC	F1	AUC	F1	AUC
Significance	***	***	***	***	**	***	***	**

On the Epinions dataset, this paper sets the proportion of rumor sources at 1%, 3%, 5%, and 7% to compare the source localization performance of various models. The experimental results are presented in Tables 5 and 6.

Table 5. The comparison among five algorithms in terms of F1-score under different proportion of rumor sources.

Proportion\Model	LPSI	GCNSI	SL-VAE	PGSL	3SGCN
1%	0.065	0.340	0.561	0.748	0.880
3%	0.057	0.236	0.487	0.726	0.879
5%	0.046	0.223	0.480	0.763	0.855
7%	0.034	0.218	0.466	0.711	0.845

Table 6. The comparison among five algorithms in terms of AUC under different proportion of rumor sources.

Proportion\Model	LPSI	GCNSI	SL-VAE	PGSL	3SGCN
1%	0.511	0.562	0.598	0.781	0.928
3%	0.438	0.510	0.624	0.819	0.943
5%	0.436	0.413	0.621	0.804	0.930
7%	0.447	0.445	0.553	0.772	0.911

The analysis of the above experimental results is as follows:

First, in terms of all metrics on all datasets, the localization performance of the 3SGCN significantly outperforms that of other comparison methods by over 10% in F1-score and over 15% in AUC on average. Notably, for the Bitcoin-OTC and Slashdot datasets, the superiority of our algorithm in localization accuracy is fully manifested. Meanwhile, for the task of multiple rumor source localization, as the number of rumor sources and infected nodes rises, the overall performance of all existing algorithms shows a decline. Nevertheless, the generalization performance of 3SGCN far surpasses that of its counterparts. It can still maintain a high level of accuracy and relative stability. This can be attributed to the fact that our algorithm combines social theory with a learning algorithm to customize the multirumor source localization framework suitable for signed social networks. Therefore, the 3SGCN algorithm can be closer to the real rumor spread scenario and further improve the accuracy and robustness of source localization even when the difficulty of the multisource localization task increases.

Second, with the growth of network size and the alteration of topological structure, the performance of all existing models drops to a certain extent. Nevertheless, in terms of multisource localization accuracy, our algorithm is proved with less reduction than other methods. It shows that the model we proposed has strong generalization. This is because this paper takes into account the characteristics of rumor dissemination in online social networks. It makes full use of the structural balance theory in social psychology to delve deeply into the intricate propagation structure formed by heterogeneous edges and integrates the characteristics of rumor centrality and source prominence to learn high-quality representations of rumor source locations. Consequently, it can effectively address the challenges posed by complex networks.

Finally, regarding different ratios of positive and negative edges, in comparison with other state-of-the-art models, the proposed algorithm demonstrates strong robustness and can still maintain a high level of source localization performance.

4.3. Ablation study

In the 3SGCN model, there are two critical modules, namely the spatial GCN module and the spectral GCN module. In order to verify the effectiveness of these two modules, four variants are designed for ablation study. Specifically, the source localization framework based on label propagation is first used as the base model. Subsequently, other modules are gradually added, including two streams merging, different paths aggregation, and signed attention mechanism. Eventually, the 3SGCN model is obtained. In this paper, the proportion of infected nodes is fixed at 25%, and a series of experiments are carried out on four real-world social networks. The contribution of each component to the overall performance is shown in Figure 6.

(1) Variant a (+ label propagation mechanism): Graph convolutional networks are applied to locate multiple rumor sources. First, features are extracted from three dimensions of positive and negative label propagation, positive label propagation only and negative label propagation only. Then, an MLP classifier is employed to determine whether each node is a rumor source or not.

(2) Variant b (+ separate processing of positive and negative subgraphs): The original graph is partitioned into positive and negative subgraphs. Graph convolution operations are carried out separately in the spectral domain for each subgraph, and then they are merged to acquire the source prominence feature of the node.

(3) Variant c (+ SI model + GAT [40]): For the infection subgraph, the unsigned SI model and unsigned graph attention network (GAT) are adopted to learn the positional representation of nodes.

(4) Variant d (+ AS-SI model + positive and negative neighbor split aggregation): Based on the AS-SI model, the representations of friends and enemies are aggregated separately from balanced and unbalanced paths and then merged to obtain the source centrality feature of nodes.

(5) Variant d (+ signed attention mechanism): Different attention weights are assigned to positive and negative neighbors on different paths.

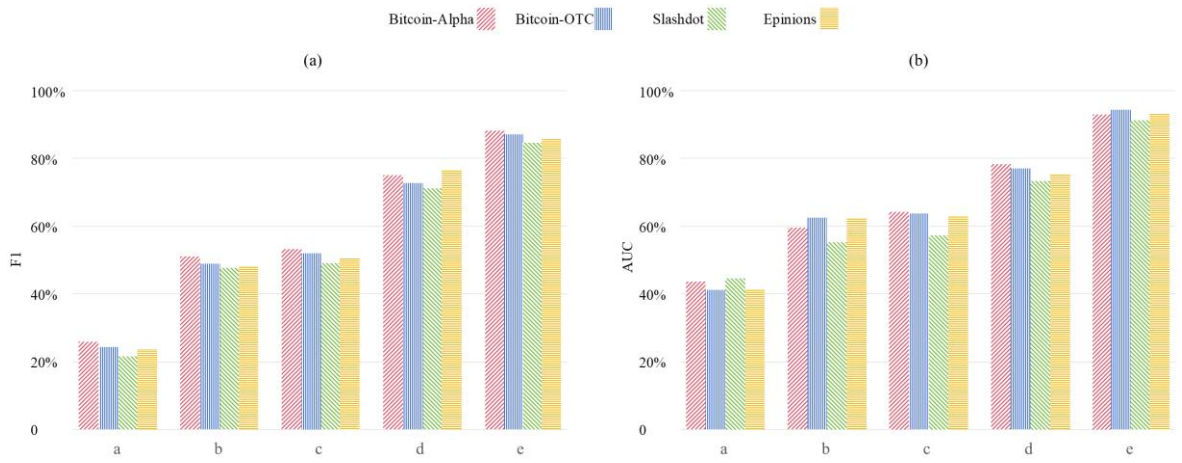

Figure 6. The performance comparison of the four variants on the following two metrics: (a) F1- score, (b) AUC. Bars of distinct colors denote the experimental outcomes on various datasets.

From the above experimental results, it can be seen that for the multisource rumor localization task, the removal of any module will lead to a decline in the overall performance of the model, which fully demonstrates the effectiveness of each component in 3SGCN. Simultaneously, different datasets exert an influence on the performance of each module, especially in large-scale networks such as Epinions and networks with more negative edges such as Slashdot, where the performance of each module generally shows a decline, but the overall impact is relatively small. This indicates that our proposed algorithm can adapt well to a variety of network types and maintain a high-level localization performance even in large-scale and complex networks.

Specifically, we first observe the contribution of variant a to the overall performance. In this paper, the GCNSI framework and MLP classifier are incorporated into the basic model, which can effectively utilize the distribution characteristics of infected and uninfected nodes for multisource localization, thus significantly improving the localization performance of the 3SGCN model. Second, when variant b is introduced to separately process positive and negative subgraphs, by mining the diverse impacts of heterogeneous edges on information dissemination, the consistent propagation structure characteristics are comprehensively extracted. As a result, the performance of the 3SGCN model is greatly enhanced. Third, after adding the unsigned graph embedding learning of variant c, although the node representations contain rich graph structure information, the ability to extract the location information of the propagation source is insufficient, and the balance of the structure composed of positive and negative edges is ignored. Therefore, the contribution of this module to the source localization performance is limited. Then, after adding variant d to the infection subgraph for branch aggregation, by encoding complex paths containing both positive and negative edges, the positive and negative neighbor embedding representations are learned, which can capture more complex propagation structure information. Therefore, this module also makes a positive contribution to the overall performance. Finally, through the incorporation of variant e's signed attention mechanism, the levels of trust in positive and negative neighbors are accurately described, which is consistent with the real-world scenarios of online network rumor propagation and is conducive to improving the accuracy of the multirumor source localization task. In summary, due to the collaborative and synergistic effects among the various modules, the proposed 3SGCN achieves the optimal performance among existing similar methods.

4.4. Parameter analysis

4.4.1. Impact of γ

In this paper, the proportion of infected nodes is fixed as 30%, and the value range of γ is set to [0.1, 0.9]. A series of experiments are conducted on four real-world datasets to observe the changes in the source localization performance of the 3SGCN model as the parameter γ increased continuously. The results are presented in Figure 7.

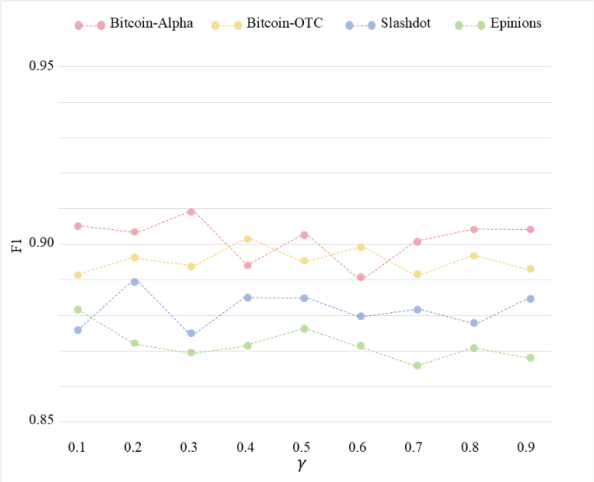

Figure 7. The impact of γ on the performance of 3SGCN algorithm. Variations in F1-scores as γ ranges from 0.1 to 0.9.

As can be seen from Figure 7, with the gradual increase of γ, the F1-score of the 3SGCN algorithm exhibits certain fluctuations yet generally remains above 0.85, indicating its excellent robustness. This is because this paper combines the complementary advantages of model-driven and data-driven approaches, integrating the spatial and spectral GCN models within a unified framework. This approach can not only give priority attention to the AS-SI propagation model but also avoid complete reliance on a specific underlying model. Without the need for prior knowledge, it strikes an effective balance between accurate modeling and uncertain diffusion. Nonetheless, for distinct datasets, there exists an optimal value of γ that maximizes the performance of the 3SGCN model. Specifically, for the Bitcoin-Alpha, Bitcoin-OTC, Slashdot, and Epinions datasets, the optimal values of γ are 0.3, 0.4, 0.2, and 0.1, respectively.

4.4.2. Impact of δ

In the spectral domain GCN module, δ is used to adjust the aggregation weights between the positive and negative streams. In this paper, the proportion of infected nodes is fixed at 30%, and extensive experiments are carried out on four real-world datasets to observe the influence of the parameter δ on the performance of the 3SGCN model. Taking the Bitcoin-Alpha dataset as an example, the experimental results are shown in Figure 8. Similar curves can also be obtained on other datasets.

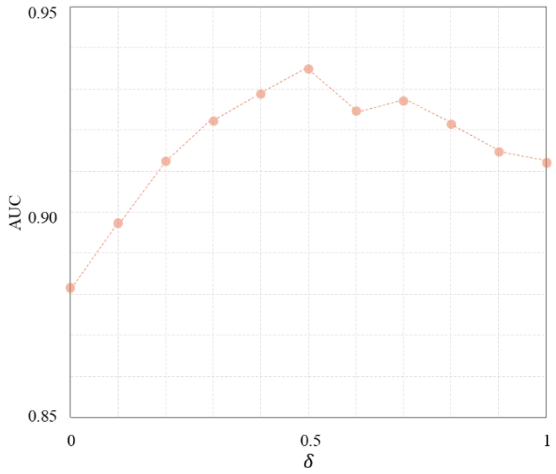

Figure 8. The impact of δ on the performance of 3SGCN algorithm. Variations in AUV values as δ ranges from 0 to 1.

As can be seen from Figure 8, when $\delta = 0.5$, the AUC value of our proposed algorithm reaches the optimum. This indicates that the positive stream is as important as the negative stream in contributing to the performance of source localization.

4.4.3. Impact of λ

In this paper, the proportion of infected nodes is fixed at 20%, and the range of λ is set to [2, 4]. Experiments are conducted on four real datasets to observe the impact of λ values on the performance of the 3SGCN model. The results are shown in Figure 9.

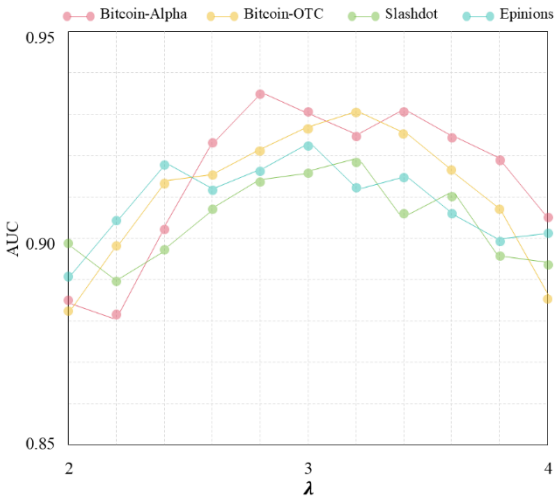

Figure 9. Performance comparison under different λ.

As can be seen from Figure 9, the value of λ has little impact on the AUC value of the algorithm proposed in this paper. Although the optimal value varies for different datasets, most of them are concentrated around the value of 3.

4.4.4. Impact of Hyperparameters

The optimal settings of the four hyperparameters, namely the number of GCN layers, the dimension of the hidden layer, the dropout rate, and the learning rate, were obtained through fivefold cross-validation. It is worth noting that when adjusting one hyperparameter, all other hyperparameters should be fixed at their optimal values. In this paper, the proportion of infected nodes was fixed at 20%. Taking the Bitcoin-Alpha dataset as an example, the F1 value of 3SGCN is shown in Figure 10.

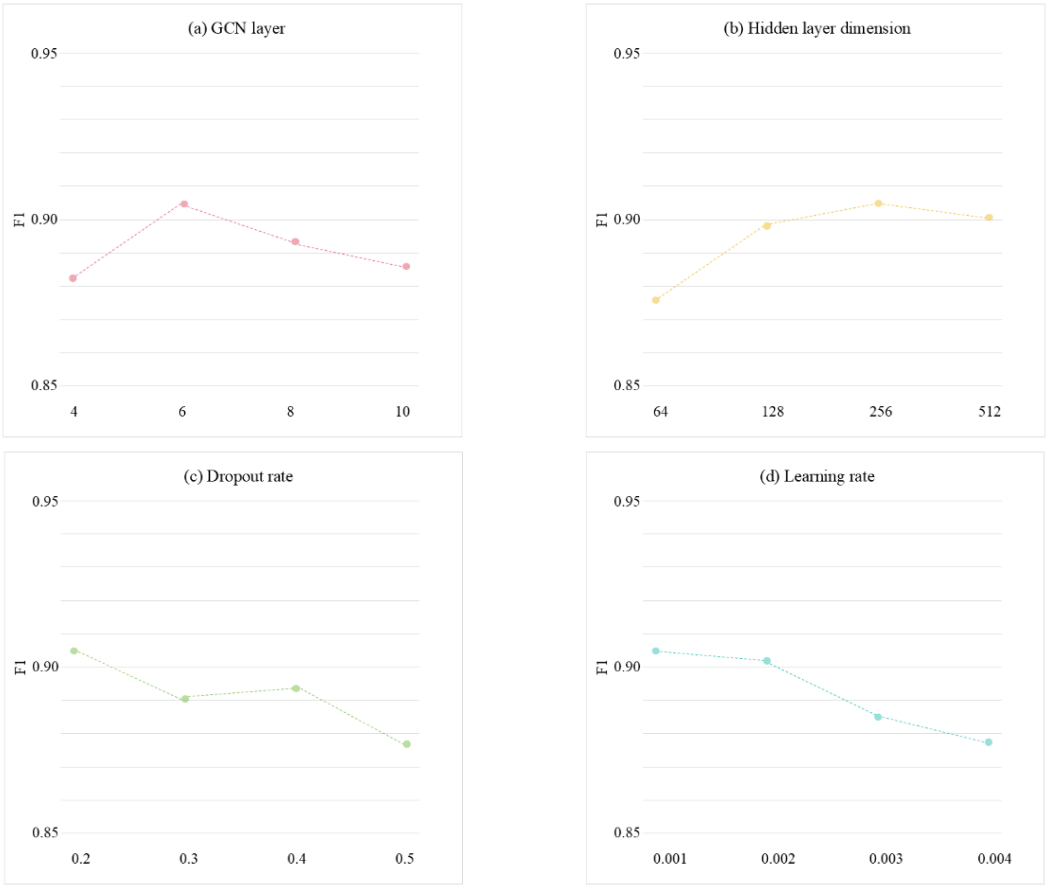

Figure 10. Performance comparison under different hyperparameters.

As can be seen from Figure 10, when 3SGCN achieves the best performance, the number of GCN layers is 6, the hidden layer dimension is 256, the dropout rate is 0.2, and the learning rate is 0.0001. This indicates that if the number of GCN layers and the hidden layer dimension are too few, it will lead to underfitting, while if they are too many, it will lead to overfitting. For the Bitcoin-Alpha dataset, an appropriate dropout rate and learning rate can further improve the performance of multisource localization. Although this paper adopts the Adam optimizer, which automatically adjusts the learning rate during training, the initial learning rate is still crucial to the training effect.

5. Conclusions

In the context of real-world online social networks, this paper proposes a multirumor source

localization framework integrating multidisciplinary approaches. First, combining social psychology theory and an epidemic model, an AS-SI propagation model suitable for signed social networks is proposed. Second, combining a complex network analysis method with a deep learning algorithm, an improved multirumor source localization algorithm that integrates spatial domain convolution and spectral domain convolution is proposed, and the rumor centrality principle and source prominence theory extend the scope to signed social networks. Upon conducting extensive experiments on four real-world social network datasets, the results demonstrate that AS-SI works very well in modeling information diffusion in signed networks, and 3SGCN can significantly outperform other comparative methods in identifying rumor initiators. At the same time, we also recognize that the overall complexity of the 3SGCN algorithm is relatively high, making it difficult to be efficiently applied to large-scale social networks. In the future, we will further enhance its operational efficiency and extend the static graph to a dynamic graph. By integrating the quasiequilibrium index and social status theory, we will construct a spatiotemporal dynamic model [41] to further improve the quality and efficiency of source localization.

Author contributions

Ying Guo: Conceptualization, data curation, formal analysis, investigation, methodology, software, writing-original draft; Yong-nan Li: Funding acquisition, project administration, resources, supervision, validation, visualization, writing-review & editing. All authors have read and approved the final version of the manuscript for publication.

Use of Generative-AI tools declaration

The authors declare that they have not used Artificial Intelligence (AI) tools in the creation of this article.

Acknowledgments

This work was supported by the Special Fund Project for Basic Scientific Research Business Expenses of Central Universities (2024JKF01) and the General Project of Intelligent Policing and National Security Risk Management Laboratory Open Research Topic (ZHKFYB2502).

Conflict of interest

The authors declare that they have no conflict of interest.

References

1. Z. X. Jiang, Z. L. Hu, F. L. Huang, Source localization in signed networks based on dynamic message passing algorithm, *Chaos Soliton. Fract.*, **188** (2024), 115532. https://doi.org/10.1016/j.chaos.2024.115532
2. A. Zubiaga, A. Aker, K. Bontcheva, M. Liakata, R. Procter, Detection and resolution of rumours in social media: A survey, *ACM Comput. Surv.*, **51** (2018), 32. https://doi.org/10.1145/3161603

3. D. Shah, T. Zaman, Rumor centrality: A universal source detector, *ACM SIGMETRICS Perform. Eval. Rev.*, **40** (2012), 199–210. https://doi.org/10.1145/2318857.2254782
4. S. S. Ali, T. Anwar, S. A. M. Rizvi, A revisit to the infection source identification problem under classical graph centrality measures, *Online Soc. Netw. Media*, **17** (2020), 100061. https://doi.org/10.1016/j.osnem.2020.100061
5. M. Li, X. Wang, K. Gao, S. S. Zhang, A survey on information diffusion in online social networks: Models and methods, *Information*, **8** (2017), 118. https://doi.org/10.3390/info8040118
6. J. Zhang, C. C. Aggarwal, P. S. Yu, Rumor initiator detection in infected signed networks, In: *Proceedings of the 37th IEEE International Conference on Distributed Computing Systems*, 2017, 1900–1909. https://doi.org/10.1109/ICDCS.2017.72
7. H. J. Li, W. Xu, S. Song, W. X. Wang, M. Perc, The dynamics of epidemic spreading on signed networks, *Chaos Soliton Fract.*, **151** (2021), 111294. https://doi.org/10.1016/j.chaos.2021.111294
8. Z. Wang, C. Wang, J. Pei, X. J. Ye, Multiple source detection without knowing the underlying propagation model, In: *Proceedings of the 31st AAAI Conference on Artificial Intelligence*, 2017. https://doi.org/10.1609/aaai.v31i1.10477
9. Z. W. Ma, H. J. Wang, Z. L. Hu, X. B. Zhu, Y. Z. Huang, F. Huang, DISLPSI: A framework for source localization in signed social networks with structural balance, *Phys. Lett. A*, **523** (2024), 129772. https://doi.org/10.1016/j.physleta.2024.129772
10. L. Qiu, S. Sai, M. Wei, BPSL: A new rumor source location algorithm based on the time-stamp back propagation in social networks, *Appl. Intell.*, **52** (2022), 8603–8615. https://doi.org/10.1007/s10489-021-02919-w
11. Z. W. Ma, L. Sun, Z. G. Ding, Y. Z. Huang, Z. L. Hu, Source localization in signed networks with effective distance, *Chin. Phys. B*, **33** (2024), 028902. https://doi.org/10.1088/1674-1056/ad1482
12. G. Baggio, D. S. Bassett, F. Pasqualetti, Data-driven control of complex networks, *Nat. Commun.*, **12** (2021), 1429. https://doi.org/10.1038/s41467-021-21554-0
13. K. Shenoy, R. Pasumarthy, V. Chellaboina, Online data-driven control of networks, In: *Proceedings of the European Control Conference*, 2024, 2985–2990. https://doi.org/10.23919/ECC64448.2024.10591319
14. P. Ji, J. C. Ye, Y. Mu, W. Lin, Y. Tian, C. Hens, et al., Signal propagation in complex networks, *Phys. Rep.*, **1017** (2023), 1–96. https://doi.org/10.1016/j.physrep.2023.03.005
15. X. L. Ru, J. M. Moore, X. Y. Zhang, Y. T. Zeng, G. Yan, Inferring patient zero on temporal networks via graph neural networks, In: *Proceedings of the 37th AAAI Conference on Artificial Intelligence*, 2023, 9632–9640. https://doi.org/10.1609/aaai.v37i8.26152
16. W. Z. Zhang, Z. Y. Liu, The influence maximization algorithm for integrating attribute graph clustering and heterogeneous graph transformer, *Heliyon*, **10** (2024), e38916. https://doi.org/10.1016/j.heliyon.2024.e38916
17. Y. D. Li, H. B. Gao, Y. X. Gao, J. X. Guo, W. L. Wu, A survey on influence maximization: From an ML-based combinatorial optimization, *ACM Trans. Knowl. Discov. Data*, **17** (2023), 133. https://doi.org/10.1145/3604559
18. M. Dong, B. Zheng, N. Q. V. Hung, H. Su, G. H. Li, Multiple rumor source detection with graph convolutional networks, In: *Proceedings of the 28th ACM International Conference on Information and Knowledge Management*, 2019, 569–578. https://doi.org/10.1145/3357384.3357994

19. C. Ling, J. J. Jiang, J. X. Wang, Z. Liang, Source localization of graph diffusion via variational autoencoders for graph inverse problems, In: *Proceedings of the 28th ACM SIGKDD Conference on Knowledge Discovery and Data Mining*, 2022, 1010–1020. https://doi.org/10.1145/3534678.3539288
20. X. Xu, T. J. Qian, Z. Xiao, N. Zhang, J. Wu, F. Zhou, PGSL: A probabilistic graph diffusion model for source localization, *Expert Syst. Appl.*, **238** (2024), 122028. https://doi.org/10.1016/j.eswa.2023.122028
21. X. Yan, H. Fang, Q. He, Diffusion model for graph inverse problems: towards effective source localization on complex networks, In: *Proceedings of the 37th International Conference on Neural Information Processing Systems*, 2023, 22326–22350.
22. D. Yan, Y. Zhang, W. Xie, Y. Jin, Y. Zhang, MUSE: Multi-faceted attention for signed network embedding, *Neurocomputing*, **519** (2023), 36–43. https://doi.org/10.1016/j.neucom.2022.11.021
23. J. Chen, Z. Wu, M. Umar, J. Yan, X. Liao, B. Tian, Learning embedding for signed network in social media with global information, *IEEE Trans. Comput. Soc. Syst.*, **11** (2024), 871–879. https://doi.org/10.1109/TCSS.2022.3217840
24. A. Gallo, D. Garlaschelli, R. Lambiotte, F. Saracco, T. Squartini, Testing structural balance theories in heterogeneous signed networks, *Commun. Phys.*, **7** (2024), 154. https://doi.org/10.1038/s42005-024-01640-7
25. M. Mueller, S. Ramkumar, Signed networks-The role of negative links for the diffusion of innovation, *Technol. Forecast. Soc. Change*, **192** (2023), 122575. https://doi.org/10.1016/j.techfore.2023.122575
26. T. Bian, X. Xiao, T. Xu, P. L. Zhao, W. B. Huang, Y. Rong, et al., Rumor detection on social media with bi-directional graph convolutional networks, In: *Proceedings of the 34th AAAI conference on artificial intelligence*, 2020, 549–556. https://doi.org/10.1609/aaai.v34i01.5393
27. F. Heider, Attitudes and cognitive organization, *J. Psychol.*, **21** (1946), 107–112. https://doi.org/10.1080/00223980.1946.9917275
28. D. Cartwright, F. Harary, Structural balance: a generalization of Heider's theory, *Psychol. Rev.*, **63** (1956), 277–293. https://doi.org/10.1037/h0046049
29. J. Kunegis, S. Schmidt, A. Lommatzsch, Spectral analysis of signed graphs for clustering, prediction and visualization, In: *Proceedings of the SIAM International Conference on Data Mining*, 2010, 559–570. https://doi.org/10.1137/1.9781611972801.49
30. Y. Xiao, G. Kang, J. Liu, B. Q. Cao, L. H. Ding, WSGCN4SLP: Weighted signed graph convolutional network for service link prediction, In: *Proceedings of the IEEE International Conference on Web Services*, 2021, 135–144. https://doi.org/10.1109/ICWS53863.2021.00029
31. Y. Wu, L. Hu, Y. Wang, Signed attention based graph neural network for graphs with heterophily, *Neurocomputing*, **557** (2023), 126731. https://doi.org/10.1016/j.neucom.2023.126731
32. T. Derr, Y. Ma, J. L. Tang, Signed graph convolutional networks, In: *Proceedings of the IEEE International Conference on Data Mining*, 2018, 929–934. https://doi.org/10.1109/ICDM.2018.00113
33. M. Schlichtkrull, T. N. Kipf, P. Bloem, R. V. D. Berg, I. Titov, M. Welling, Modeling relational data with graph convolutional networks, In: *Proceedings of the European Semantic Web Conference*, 2018, 593–607. https://doi.org/10.1007/978-3-319-93417-4_38

34. C. X. He, J. Y. Zeng, Y. Li, S. T. Liu, L. L. Liu, C. Xiao, Two-stream signed directed graph convolutional network for link prediction, *Physica A*, **605** (2022), 128036. https://doi.org/10.1016/j.physa.2022.128036
35. T. N. Kipf, M. Welling, Semi-supervised classification with graph convolutional networks, In: *Proceedings of the 5th International Conference on Learning Representations*, 2017, 1–14.
36. S. Kumar, F. Spezzano, V. Subrahmanian, C. Faloutsos, Edge weight prediction in weighted signed networks, In: *Proceedings of the 16th IEEE International Conference on Data Mining*, 2016, 221–230. https://doi.org/10.1109/ICDM.2016.0033
37. J. Leskovec, D. Huttenlocher, J. Kleinberg, Signed networks in social media, In: *Proceedings of the 28th ACM Conference on Human Factors in Computing Systems*, 2010, 1361–1370. https://doi.org/10.1145/1753326.1753532
38. A. Paszke, S. Gross, S. Chintala, G. Chanan, E. Yang, Z. DeVito, et al., Automatic differentiation in pytorch, In: *Proceedings of the 31st International Conference on Neural Information Processing Systems*, 2017, 1–4. https://openreview.net/forum?id=BJJsrmfCZ
39. M. Fey, J. E. Lenssen, Fast graph representation learning with PyTorch Geometric, 2019, arXiv: 1903.02428v3. https://doi.org/10.48550/arXiv.1903.02428
40. P. Veličković, G. Cucurull, A. Casanova, A. Romero, P. Liò, Y. Bengio, Graph attention networks, 2018, arXiv:1710.10903v3. https://doi.org/10.48550/arXiv.1710.10903
41. L. Zhu, T. Zheng, Pattern dynamics analysis and application of West Nile virus spa-tiotemporal models based on higher-order network topology, *Bull. Math. Biol.*, **87** (2025), 121. https://doi.org/10.1007/s11538-025-01501-6

AIMS Press